Biogeosciences Discuss., https://doi.org/10.5194/bg-2018-380
Manuscript under review for journal Biogeosciences
Discussion started: 13 September 2018

Methane emissions from a sediment-deposited island in a Lancang-Mekong reservoir

Wenqing Shi[1,2], Qiuwen Chen[1,2], Jianyun Zhang[1,3], Cheng, Chen[2], Yuchen Chen[2],Yuyu Ji[2,4], Juhua Yu[1,2], Bryce R. Van Dam[5]

[1]State Key Laboratory of Hydrology-Water Resources & Hydraulic Engineering, Nanjing Hydraulic Research Institute, China

[2]Center for Eco-Environment Research, Nanjing Hydraulic Research Institute, China

[3]Research Center for Climate Change, Ministry of Water Resources, China

[4]College of Water Conservancy and Hydropower Engineering, Hohai University, China

[5]Institute of Marine Sciences, University of North Carolina at Chapel Hill, USA

Correspondence to: Qiuwen Chen (qwchen@nhri.cn)

Abstract

In dammed rivers, sediment accumulation creates potential methane emission hotspots, which have been extensively studied in forebays. However, methane emissions from sidebays remain poorly understood. We investigated methane emissions from a sediment-deposited island situated in the sidebay of the Manwan Reservoir, Lancang-Mekong River. High methane emissions (maximum 10.4 mg $h^{-1}m^{-2}$) were observed at the island center, while a ring-like zone of low-to-negative methane emission was discovered around the island edge, whose flux varied between -0.2–1.6 mg $h^{-1}m^{-2}$. The ring-like zone accounted for 89.1 % of the island area, of which 9.1 % was a methane sink zone. Microbial processes in the hyporheic zone, regulated by hydrological variations, were responsible for the low methane flux in this area. Under reservoir operation, frequent water level fluctuations enhanced hyporheic exchange and created redox gradients along the hyporheic flow path. Dissolved oxygen in hyporheic water decreased from 4.80 mg L^{-1} at the island bank edge to 0.43 mg L^{-1} at the center, which in turn decreased methanogen abundance for methane production and increased methanotroph abundance for methane oxidation at the ring-like zone. This study quantified the methane emissions from sediment deposited islands in the reservoir and helps to evaluate the global warming effects of hydropower systems.

Biogeosciences Discuss., https://doi.org/10.5194/bg-2018-380
Manuscript under review for journal Biogeosciences
Discussion started: 13 September 2018

1 Introduction

Natural rivers form continuous ecosystems, in which physical and chemical factors drive biological processes from headwaters to river deltas (Butman and Raymond, 2011; Wilkinson et al., 2015). Along this continuum, rivers receive terrestrial organic carbon (OC) and deliver it to the ocean at a global average rate of approximately 400–900 Tg OC per year (Butturini et al., 2016; Seitzinger et al., 2005; Ran et al., 2013). In the past two decades, many rivers have become intensively regulated by dams for a variety of purposes, including improved navigation, water supply, flood control, and hydropower production (Maavara et al., 2015). These engineering works decrease water velocity, converting rivers into a series of lentic reservoirs, where sediment accumulates in forebays and sidebay islands (Maeck et al., 2013). Globally, the sediment accumulation process has reduced the river-to-ocean flux of terrestrial OC by 26 % (Syvitski et al., 2005).

Settling particles aggregate to form cohesive sediment layers, which often become anoxic after oxygen is consumed but not replenished through diffusive exchange (Rubol et al., 2013; Maeck et al., 2013). Subsequently, large amounts of methane may be produced and released into the atmosphere (Thornton et al., 1990; Maeck et al., 2013; Wilkinson et al., 2015), thereby reducing the green credentials of hydropower. This issue has received considerable attention in dammed rivers (Giles, 2006; Hu and Cheng, 2013). Maeck et al. (2013) identified reservoirs as methane emission hotspots by comparing reservoir and riverine reaches, and estimated that global methane emissions have increased by 7 % due to sedimentation in dammed rivers. In sidebays, the deposited sediments often form hyporheic zones, where water, heat, nutrients and chemicals are exchanged and many biogeochemical reactions preferentially occur (Tonina and Buffington, 2011; Cardenas and Markowski, 2010), potentially emitting large amounts of greenhouse gases. Previous studies have mainly focused on methane emissions from dam forebays (Yang et al., 2013; DelSontro et al., 2010; DelSontro et al., 2011), while the understandings of methane emissions from sediments deposited in sidebays remain poor.

In reservoirs, frequent water level fluctuations often occur following hydropower production demands, which enhances hyporheic exchange by driving water flow in and out of reservoir sidebays (Tonina and Buffington, 2011; Hucks Sawyer et al., 2009). This may lead to changes in the redox conditions of sidebay sediments. Zarnetske found a redox gradient along the hyporheic flow paths in a third-order stream in the Willamette River basin, USA (Zarnetske et al., 2011a). Methane from sediments is mainly produced by anaerobic methanogens, and is consumed by aerobic methanotrophs (Borrel et al., 2011). We suppose the shift in sediment redox conditions may affect the microbial processes, thereby altering the methane emission scheme.

In this study, methane emissions from a sediment-deposited island were investigated in the sidebay of Manwan Reservoir, Lancang-Mekong River. Monitoring wells were established to probe hyporheic exchange and redox gradients across the island. Methanogen and methanotroph abundances in the sediment were analyzed using quantitative polymerase chain reaction (qPCR) to reveal the associated molecular mechanism. The objective of this study was to explore methane emissions from sediment-deposited zones in a sidebay of a dammed river, with the goal to guide future mitigation of the global warming effects of hydropower development.

2 Methods

2.1 Study area

The Lancang-Mekong River, a trans-boundary river in Southeast Asia, originates from the Tibetan Plateau and discharges into the South China Sea. It has a length of 4909 km, a watershed area of 760,000 km^2, and a mean annual runoff of 457 km^3 at a discharge of 14,500 m^3 s^{-1} (Li et al., 2013). The Lancang-Mekong Basin can be divided into two parts: the "upper basin" in China, and the "lower basin" from Yunnan in China to the Southeast Asia. Until now, seven dams have been built for hydropower production in the upper Lancang-Mekong River in China, including Miaowei, Gongguoqiao, Xiaowan, Manwan, Dachaoshan, Nuozhadu and Jinghong. The locations and main features of these dams were shown in Fig. 1 and Table S1 in the Supplements, respectively.

After impoundment, several different types of islands formed in the reservoir (Fig. S1). This study selected a typical island for investigation (182 m in length, 90 m in width), which is located at the convex bank (24°43′44″ N, 100°23′5″ E) in the sidebay of Manwan reservoir, 30 km away from the dam (Fig. 1). Manwan has a subtropical plateau monsoon climate, featuring no distinct seasons. Under reservoir operation, the island bank is frequently flooded (Fig. S2).

2.2 Monitoring wells

Ten monitoring wells were installed in the island bank at 0.5 (W1), 1.5 (W2), 3.5 (W3),

Biogeosciences Discuss., https://doi.org/10.5194/bg-2018-380
Manuscript under review for journal Biogeosciences
Discussion started: 13 September 2018

6.5 (W4), 10.5 (W5), 15.5 (W6) 20.5 (W7), 25.5 (W8), 30.5 (W9), and 35.5 m (W10) from the waterline, respectively (Fig. S2). The wells were 90-mm diameter perforated polyvinylchloride pipes, reaching a depth of 2.0 m below the ground surface. To prevent flooding, the wells were extended 2.0 m aboveground. Due to hydropower production, the reservoir runs in a pseudo-periodic hydrological regime with cyclic water level fluctuations. Here, we monitored a complete cycle of water level fluctuation within 115 h. Water levels were measured every 10 min from 11 to 16 September 2016 using automated water level recorders (U2000101, OneSetHoBo, USA), which were mounted at the bottom of W5, W7, W10, and the reservoir (Fig. S3).

Instantaneous lateral fluid fluxes (*q*) across the island bank per unit length were calculated following the Darcy Eq. (1) (Gerecht et al., 2011; Hucks Sawyer et al., 2009):

$$q(t) = -Kb \cdot \left[\frac{\vartheta h(x,t)}{\vartheta x}\right] \quad (1)$$

where *Kb* is sediment transmissivity, m d^{-1}; *h* is hydraulic head, m; *x* is distance, m; and *t* is time, d. A positive *q* value indicates flow from the reservoir to the island. The island *Kb* was 0.99 m d^{-1}, which was measured according to Philip (1993).

2.3 Sampling and physicochemical analysis

After water level receded at the monitoring time of 100 h, groundwater (100 ml) was carefully sampled in triplicate from each monitoring well with a portable peristaltic pump (SC-1/253Yx, Chongqing Jieheng Peristaltic Pump Co., Ltd., China), and then filtered *in situ* using portable syringe filters for water DOC analysis. Sediment (5 g) was synchronously collected in triplicate from 10 cm below the surface adjacent to each well using a hand shovel, and then homogenized before the storage for the analyses of sediment OC and microbe. At a reservoir site adjacent to W1, water and surface sediment samples were also collected in triplicate using a stainless-steel bucket and an Ekman grab sampler, respectively. The collected water and sediment samples were kept frozen in an ice box (-5 ℃–-10 ℃) and transported to the laboratory for analysis within three days.

Water temperature (WT), dissolved oxygen (DO), pH, and electrical conductivity (EC) at each well were measured *in situ* using a multi-sensor probe (YSI 6600, Yellow Springs Instruments, USA). Analysis of dissolved organic carbon (DOC) in the water was conducted on filtered samples (Whatman GF/F, UK) using a total organic carbon analyzer (Liqui TOC II, Elementar Inc., Germany). Sediment OC was determined using a vario MACRO cube elementar (Elementar Inc., Germany). Fresh sediment was freeze-dried and ground before analysis. Approximately 30 mg of each sample was weighed in a tin cup and acidified with two drops of 8 % H_3PO_4 to remove inorganic carbonates before OC analysis.

2.4 Methane flux analysis

Methane fluxes from the reservoir (eight sampling sites) and island (seventeen sampling sites) were analyzed using bifunctional chambers according to the static chamber method (Duchemin et al., 1999). The sampling sites are shown in Fig. S4. The plexiglass bifunctional chamber consisted of a 6.28-L cylinder (20 cm in diameter, 20 cm in height) and a removable Styrofoam collar. During gas collection in the reservoir, the chamber was fitted with the Styrofoam collar, which maintained the upper closed portion of the chamber about 10 cm above the water surface (Fig. S5). The chambers were left to stand for 20 min before sample collection. Gas samples (20 ml) were collected every 10 min over a 40-min period using a 25-ml polypropylene syringe and injected into a pre-evacuated Exetainer® vial (839 W, Labco, UK) for storage until analysis using a gas chromatograph (7890B, Agilent Technologies, USA). Gas fluxes were calculated using linear regression based on the concentration changes of five samples over time. Linear regression correlation coefficients of less than 0.95 were not accepted for further calculations (Duchemin et al., 1999). Simple spline interpolation was used to interpolate the methane emissions from the sampling sites into space in the reservoir and island separately (Immerzeel et al., 2009). Methane emission areas at eight different categories were also calculated in the island.

2.5 Microbial abundance analysis

After being transported to the laboratory, the frozen sediment samples were stored immediately at -80 ℃ for further molecular analysis. The sediment methanogens and methanotrophs adjacent to each monitoring well across the island (ten sediment samples) were quantified using qPCR. DNA extraction was undertaken using a FastDNA Power-Max Soil DNA Isolation Kit (MP Biomedical, USA) according to the manufacturer's instructions. The qPCR assay was performed using primers targeting methanogenic archaeal 16S rDNA (primer set, 1106F/1378R) and methanotrophic *pmoA* genes (primer set, A189F/M661R) (Watanabe et al., 2007; Ma and Lu, 2011). Gene copies were amplified and quantified in a Bio-Rad cycler equipped with the iQ5 real-time fluorescence detection system and software (version 2.0, Bio-Rad, USA). All reactions were completed in a total volume of 20 μL containing 10 μL SYBR® *Premix Ex Taq*™

(Toyobo, Japan), 0.5 mM of each primer, 0.8 μL of BSA (3 mg mL^{-1}, Sigma, USA), ddH_2O, and template DNA. The qPCR program for archaeal 16S rDNA was as follows: 95 ℃ for 60 s, followed by 40 cycles of 95 ℃ for 25 s, 57 ℃ for 30 s, and 72 ℃ for 60 s. The qPCR program for *pomA* commenced with 95 ℃ for 60 s, followed by 40 cycles of 95 ℃ for 25 s, 53 ℃ for 30 s, and 72 ℃ for 60 s. A standard curve was established by serial dilution (10^{-2}–10^{-8}) of known concentration plasmid DNA with the target fragment. All PCRs were run in triplicate on 96-well plates (Bio-Rad, USA) sealed with optical-quality sealing tape (Bio-Rad, USA). Three negative controls without the DNA template were included for each PCR run.

2.6 Data analysis

One-way analysis of variance (ANOVA) was employed to test the statistical significance of differences between sampling sites. Post-hoc multiple comparisons of treatment means were performed using the Tukey's least significant difference procedure. All statistical calculations were performed using the SPSS (v22.0) statistical package for personal computers. The level of significance was $P < 0.05$ for all tests.

3 Results

3.1 Physicochemical characteristics

As shown in Fig. 2, the island groundwater had lower DO and pH, but higher WT, EC, and DOC, compared with that of the bulk reservoir water. Lateral gradients of groundwater pH and DO, and DOC were observed in the island. From the island edge to the center, pH gradually increased from 6.55 ± 0.13 to 7.25 ± 0.12, whereas DO and DOC decreased significantly from 4.80 ± 0.19 to 0.43 ± 0.09 mg L^{-1} and 7.30 ± 0.54 to

1.70 ± 0.39 mg L^{-1}, respectively (P < 0.05). There were no significant differences in WT or DO between sampling sites (P > 0.05), which ranged from 15.9–17.4 °C and 390–761 μS cm^{-1}, respectively (Fig. 2a-e). In general, sediment OC was higher near the island edge, decreasing from 6.37 ± 0.69 mg g^{-1} at the edge to 2.42 ± 0.60 mg g^{-1} at the center of the island. Sediment OC in the reservoir was 6.63 ± 0.09 mg g^{-1} (Fig. 2e).

3.2 Water level fluctuation and hyporheic exchange

The reservoir stage fluctuated frequently during the field survey, showing three distinct peaks, with a maximum of 3.80 m in the first 37 h and gradual decline to below 1.30 m in the next 60 h, yielding a maximum oscillation of 2.54 m. Similar oscillations were observed in the island water table, but were damped and lagged relatively to the reservoir stage fluctuations (Fig. 3a). In W5, W7, and W10, the water levels reached 3.27, 3.41, and 3.33 m, then fell to 1.74, 2.09, and 2.01 m, for a maximum oscillation of 1.53, 1.33, and 1.32 m, respectively. Data from the automated water level recorders indicated that the water level responses in W5, W7, and W10 lagged the reservoir stage by 20, 25, and 30 min, respectively. Lateral hyporheic exchanges across the island bank were calculated according to the Darcy Law, showing that the flux was largest at the island edge and decreased from the edge to the center. The water exchange across the 0–10.5 m island edge zone was 1.2 and 4.7 times higher than those across the 10.5–20.5 m and 20.5–35.5 m zones, respectively. The flow rates at the reservoir-W5, W5-W7, and W7-W10 zones were relatively consistent at -0.55–1.35, -0.89–0.28, and -0.39–0.17 m^2 d^{-1} (Fig. 3b), resulting in a water exchange volume of 2.61, 2.26, and 0.56 m^3, respectively, over the 115-h observation period.

3.3 Methane emissions

High methane emission rates were observed at the island sites, with a maximum of 10.4 mg $h^{-1}m^{-2}$ at the center. However, a large ring-like low methane emission zone appeared around the island edge, where the methane flux was maintained at -0.2–1.6 mg $h^{-1}m^{-2}$ (Fig. 4a). The negative flux values also suggest the occurrence of a methane sink at the island edge. The ring-like zone accounted for 89.1 % of the island area, of which 9.1 % accounted for the methane sink zone (Fig. 4b). Compared with the island, the methane flux from the adjacent reservoir was moderate at 0.4–5.5 mg $h^{-1}m^{-2}$ (Fig. 4a).

3.4 Methanogen and methanotroph abundances

Methanogens and methanotrophs were distributed non-uniformly across the island. In general, methanogen counts were low at the island edge but high at the center, whereas methanotrophs were abundant at the island edge but scarce in the center. From the island edge to the center, the methanogenic archaeal 16S rDNA gene increased from 0.12×10^5 to 5.34×10^5 copies g^{-1}, and the methanotrophic *pmoA* gene decreased from 1.57×10^6 to 0.64×10^6 copies g^{-1}.

4 Discussion

4.1 Hyporheic exchange and redox gradients

The hyporheic zone is the interface beneath and adjacent to streams and rivers, where water, heat, nutrients and contaminants are exchanged and many biogeochemical reactions occur (Cardenas and Markowski, 2010; Tonina and Buffington, 2011). In hydropower reservoirs, the release of water pulses is often employed to increase power production and meet daily electricity peak demand (Bonalumi et al., 2012; Toffolon et al., 2010). Such hydropeaking creates daily water level fluctuations in the reservoir. In this study, frequent water level fluctuations were observed within the 115-h observation period, with a maximum of 3.80 m (Fig. 3a). A hysteretic response occurred in the island bank water table (Fig. 3a), driving water exchange between the reservoir and island (Fig. 3b). The water exchange flux was largest close to the island edge and decreased from the edge to the center, as water table fluctuations were attenuated (Fig. 3a).

During a storage-release cycle, the island switched from water gaining to losing at daily or hourly scales, creating a ring-like zone of enhanced hyporheic exchange around the island. The hyporheic zone extended tens of meters into the island bank (Fig. 3b). If the river system was unregulated, however, hydrodynamics within the hyporheic zone would likely exhibit seasonal or annual patterns, or keep pace with snowmelt and rainstorm events, under a natural base flow-fed regime. In this case, hyporheic zones may be limited or altogether absent (Boano et al., 2008; Cardenas and Wilson, 2007).

Exchange across the sediment-water interface involves mixing of surface water and groundwater through hyporheic flow (Hester et al., 2013; Naranjo et al., 2015). In this study, when the reservoir water entered the hyporheic flow path, it was typically rich in oxygen (Fig. 2d). As oxygen was consumed through aerobic respiration, other terminal electron acceptors were utilized (Klupfel et al., 2014), creating a redox gradient along the hyporheic flow path (Fig. 2d). Changes in sediment moisture can speed up the mineralization of organic matter (Wang et al., 2010; Rubol et al., 2014). Groundwater DOC showed a general decrease from the island edge to center (Fig. 2e). This hyporheic exchange clearly affected biogeochemical processes, and had important effects on hyporheic microbial communities, especially redox-sensitive species. For example, we detected poor methanogen abundance at the island edge, but rich abundance at the center, with methanotrophs showing the opposite pattern (Fig. 5). The spatial heterogeneity of sediment OC in the island was likely due to the settled particles with different organic matter contents during the island formation, or the release of the exudates from benthic biofilms, including algae and other primary producers, under hyporheic exchanges (Rubol et al., 2014).

4.2 Self-mitigation of methane emissions

Methane is the second most important greenhouse gas, contributing approximately 18 % to total global warming effects (Smith et al., 2013; Wuebbles and Hayhoe, 2002). Inland waters (lakes, rivers, and reservoirs) are significant sources of atmospheric methane, which is mainly released from anoxic sediment (Bastviken et al., 2011; Sobek et al., 2012). In dammed rivers, riverbed sediment accumulation in forebays and sidebay islands creates potential methane emission hotspots. In this study, however, high methane emissions were only observed at the island center, with a ring-like low methane emission zone or even methane sink appearing around the island edge (Fig. 4a). In natural waters, methane is primarily produced by methanogens under anaerobic conditions (Yang et al., 2017). Along the redox gradient in the island (Fig. 2d), methane production was inhibited at the edge and favored at the center, as indicated by the lower abundance of sediment methanogens at the island edge than at the center (Fig. 5). The methane sink at the island edge was mainly attributed to oxidation consumption by methanotrophs. The aerobic sediment at the island edge was rich in methanotrophs (Fig. 5), which may consume methane to below equilibrium with the atmosphere, driving a net air-water flux. Groundwater DOC and sediment OC at the island edge, which are carbon sources for methane emission, were higher than that at the island center (Fig. 2e,f), suggesting that both sediment heterogeneity and dilution effects of hyporheic exchange had limited contribution to the spatial pattern of methane emissions in the island. Hyporheic exchange effectively shifted redox gradients across the island, resulting in substantial mitigation of potential methane emissions. In this study, only 0.2 % of the island area maintained a high methane flux (9.6–11.2 mg $h^{-1}m^{-2}$) (Fig. 4b), suggesting that methane emissions across the small island were attenuated, but only in the area where hyporheic exchange occurred. It may be possible for methane emission hotspots in larger islands to be mitigated by enlarging their hyporheic zone. For example, artificial channels can be made through the island to create a hyporheic zone in the center (Fig. S6). In addition, the maximum water level in the reservoir can be raised by modifying hydropower operation scenarios to extend the hyporheic zone (Fig. S6).

4.3 Implications

Greenhouse gas emissions significantly detract from the green credentials of hydropower, and have thus received considerable research attention (Giles, 2006; Hu and Cheng, 2013). Previous studies have revealed that damming causes significant retention of carbon and creates deep, anoxic sediment strata, fueling methanogenesis and net water-air methane flux (Maeck et al., 2013). In this study, the self-mitigation of methane emissions was apparent in the hyporheic zone under the reservoir operations. Given the widely distributed hyporheic zones in reservoirs, this self-mitigation should be of concern in future estimations of greenhouse gas emissions from dammed rivers. Prospective studies should assess the quantitative relationship between methane emissions from the hyporheic zone and hydropower operation scenarios.

Until now, few studies have concentrated on organic carbon mineralization in the hyporheic zone of reservoirs, with most focusing on the process of denitrification (Zarnetske et al., 2011b). Carbon emissions in the hyporheic zone are poorly understood, especially in regulated and dammed rivers. This study fills the knowledge gap and adds to our understanding of the ecological impacts of hydropower exploitation. Under reservoir operation, variable redox conditions and methane production may also affect the mercury cycle in the hyporheic zone and thereby the release of methylmercury (a bioaccumulative environmental toxicant) to the river (Marvin-DiPasquale et al., 2009), a subject deserving of further study.

The methods used in this study had some limitations. First, an average value of hydraulic conductivity was chosen for calculating the Darcy fluxes, which does not reflect the full heterogeneity of island sediment, which ranges from silt and fine clay to sand. Second, direct measurements in the open monitoring wells introduced atmospheric oxygen into the previously isolated groundwater, presenting possible systematic errors in the groundwater data. However, even with these potential complications, the data obtained in the present study were useful for clarifying the biogeochemical processes in the hyporheic zone associated with reservoir operation.

Biogeosciences Discuss., https://doi.org/10.5194/bg-2018-380
Manuscript under review for journal Biogeosciences
Discussion started: 13 September 2018

5 Conclusions

In dammed rivers, sediment deposited islands are widely distributed in sidebays and are potential hotspots of methane emission to the atmosphere. In this study, high methane fluxes were only observed at the island center, while a ring-like zone of low methane emission or even sink was found around the island edge. We attribute this methane mitigation to hyporheic exchange between the reservoir and island. Under reservoir operation, frequent water level fluctuations drove hyporheic exchange, creating redox gradients along the hyporheic flowpath. These redox gradients affected the microbial communities associated with methane production and consumption, producing a net effect of methane emission self-mitigation. Our understanding of this self-mitigation of methane emission in dammed rivers will help us to screen effective strategies seeking to lessen the global warming impacts of hydropower systems.

Data availability

The data presented here can be obtained upon request to Wenqing Shi (wqshi@nhri.cn).

Author contribution

Qiuwen Chen designed the research; Wenqing Shi, Yuyu Ji and Yuchen Chen performed the research; Cheng Chen and Juhua Yu contributed new reagents/analytic tools; Qiuwen Chen and Wenqing Shi analyzed the data; Jianyun Zhang and Bryce R. Van Dam contributed significant discussions and inputs; Wenqing Shi and Qiuwen Chen wrote the paper with input from all authors.

Competing interests

The authors declare that they have no conflict of interest.

Acknowledgements

Funding for this study was provided by the National Nature Science Foundation of China (No. 91547206, 51425902, 51709181 and 51709182).

Biogeosciences Discuss., https://doi.org/10.5194/bg-2018-380
Manuscript under review for journal Biogeosciences
Discussion started: 13 September 2018

References

Bastviken, D., Tranvik, L. J., Downing, J. A., Crill, P. M., and Enrich-Prast, A.: Freshwater methane emissions offset the continental carbon sink, Science, 331, 50-50, 10.1126/science.1196808, 2011.

Boano, F., Revelli, R., and Ridolfi, L.: Reduction of the hyporheic zone volume due to the stream-aquifer interaction, Geophys. Res. Lett., 35, 2008.

Bonalumi, M., Anselmetti, F. S., Wüest, A., and Schmid, M.: Modeling of temperature and turbidity in a natural lake and a reservoir connected by pumped-storage operations, *Water Resour. Res.*, 48, 10.1029/2012wr011844, 2012.

Borrel, G., Jezequel, D., Biderre-Petit, C., Morel-Desrosiers, N., Morel, J. P., Peyret, P., Fonty, G., and Lehours, A. C.: Production and consumption of methane in freshwater lake ecosystems, Res Microbiol, 162, 832-847, DOI 10.1016/j.resmic.2011.06.004, 2011.

Butman, D., and Raymond, P. A.: Significant efflux of carbon dioxide from streams and rivers in the United States, Nature Geoscience, 4, 839-842, 2011.

Butturini, A., Guarch, A., Romaní, A., Freixa, A., Amalfitano, S., Fazi, S., and Ejarque, E.: Hydrological conditions control in situ DOM retention and release along a Mediterranean river, Water research, 99, 33-45, 2016.

Cardenas, M. B., and Wilson, J. L.: Exchange across a sediment-water interface with ambient groundwater discharge, Journal of hydrology, 346, 69-80, 2007.

Cardenas, M. B., and Markowski, M. S.: Geoelectrical imaging of hyporheic exchange and mixing of river water and groundwater in a large regulated river, Environmental

Biogeosciences Discuss., https://doi.org/10.5194/bg-2018-380
Manuscript under review for journal Biogeosciences
Discussion started: 13 September 2018

Science & Technology, 45, 1407-1411, 2010.

DelSontro, T., McGinnis, D. F., Sobek, S., Ostrovsky, I., and Wehrli, B.: Extreme methane emissions from a Swiss hydropower reservoir: contribution from bubbling sediments, Environmental science & technology, 44, 2419-2425, 2010.

DelSontro, T., Kunz, M. J., Kempter, T., Wüest, A., Wehrli, B., and Senn, D. B.: Spatial heterogeneity of methane ebullition in a large tropical reservoir, Environmental science & technology, 45, 9866-9873, 2011.

Duchemin, E., Lucotte, M., and Canuel, R.: Comparison of static chamber and thin boundary layer equation methods for measuring greenhouse gas emissions from large water bodies §, Environmental Science & Technology, 33, 350-357, 1999.

Gerecht, K. E., Cardenas, M. B., Guswa, A. J., Sawyer, A. H., Nowinski, J. D., and Swanson, T. E.: Dynamics of hyporheic flow and heat transport across a bed-to-bank continuum in a large regulated river, Water Resources Research, 47, 2011.

Hester, E. T., Young, K. I., and Widdowson, M. A.: Mixing of surface and groundwater induced by riverbed dunes: Implications for hyporheic zone definitions and pollutant reactions, Water Resources Research, 49, 5221-5237, 10.1002/wrcr.20399, 2013.

Hu, Y., and Cheng, H.: The urgency of assessing the greenhouse gas budgets of hydroelectric reservoirs in China, Nature Climate Change, 3, 708, 2013.

Hucks Sawyer, A., Bayani Cardenas, M., Bomar, A., and Mackey, M.: Impact of dam operations on hyporheic exchange in the riparian zone of a regulated river, Hydrol Process, 23, 2129-2137, 2009.

Immerzeel, W., Rutten, M., and Droogers, P.: Spatial downscaling of TRMM precipitation using vegetative response on the Iberian Peninsula, Remote Sens Environ, 113, 362-370, 2009.

Klupfel, L., Piepenbrock, A., Kappler, A., and Sander, M.: Humic substances as fully regenerable electron acceptors in recurrently anoxic environments, Nat Geosci, 7, 195-200, 10.1038/NGEO2084, 2014.

Li, J. P., Dong, S. K., Liu, S. L., Yang, Z. F., Peng, M. C., and Zhao, C.: Effects of cascading hydropower dams on the composition, biomass and biological integrity of phytoplankton assemblages in the middle Lancang-Mekong River, Ecol Eng, 60, 316-324, 10.1016/j.ecoleng.2013.07.029, 2013.

Ma, K., and Lu, Y.: Regulation of microbial methane production and oxidation by intermittent drainage in rice field soil, Fems Microbiol Ecol, 75, 446-456, 10.1111/j.1574-6941.2010.01018.x, 2011.

Maavara, T., Parsons, C. T., Ridenour, C., Stojanovic, S., Durr, H. H., Powley, H. R., and Van Cappellen, P.: Global phosphorus retention by river damming, P Natl Acad Sci USA, 112, 15603-15608, 10.1073/pnas.1511797112, 2015.

Maeck, A., DelSontro, T., McGinnis, D. F., Fischer, H., Flury, S., Schmidt, M., Fietzek, P., and Lorke, A.: Sediment trapping by dams creates methane emission hot spots, Environmental Science & Technology, 47, 8130-8137, 10.1021/es4003907, 2013.

Marvin-DiPasquale, M., Lutz, M. A., Brigham, M. E., Krabbenhoft, D. P., Aiken, G. R., Orem, W. H., and Hall, B. D.: Mercury cycling in stream ecosystems. 2. Benthic methylmercury production and bed sediment-pore water partitioning, Environmental science & technology, 43, 2726-2732, 2009.

Biogeosciences Discuss., https://doi.org/10.5194/bg-2018-380
Manuscript under review for journal Biogeosciences
Discussion started: 13 September 2018

Naranjo, R. C., Niswonger, R. G., and Davis, C. J.: Mixing effects on nitrogen and oxygen concentrations and the relationship to mean residence time in a hyporheic zone of a riffle-pool sequence, Water Resources Research, 51, 7202-7217, 10.1002/2014WR016593, 2015.

Philip, J.: Approximate analysis of falling-head lined borehole permeameter, Water Resources Research, 29, 3763-3768, 1993.

Ran, L., Lu, X., Sun, H., Han, J., Li, R., and Zhang, J.: Spatial and seasonal variability of organic carbon transport in the Yellow River, China, Journal of Hydrology, 498, 76-88, 2013.

Rubol, S., Manzoni, S., Bellin, A., and Porporato, A.: Modeling soil moisture and oxygen effects on soil biogeochemical cycles including dissimilatory nitrate reduction to ammonium (DNRA), Advances in water resources, 62, 106-124, 2013.

Rubol, S., Freixa, A., Carles-Brangari, A., Fernàndez-Garcia, D., Romaní, A., and Sanchez-Vila, X.: Connecting bacterial colonization to physical and biochemical changes in a sand box infiltration experiment, Journal of hydrology, 517, 317-327, 2014.

Seitzinger, S., Harrison, J., Dumont, E., Beusen, A. H., and Bouwman, A.: Sources and delivery of carbon, nitrogen, and phosphorus to the coastal zone: An overview of Global Nutrient Export from Watersheds (NEWS) models and their application, Global Biogeochem Cy, 19, 2005.

Smith, K. R., Desai, M. A., Rogers, J. V., and Houghton, R. A.: Joint CO_2 and CH_4 accountability for global warming, Proceedings of the National Academy of Sciences,

Biogeosciences Discuss., https://doi.org/10.5194/bg-2018-380
Manuscript under review for journal Biogeosciences
Discussion started: 13 September 2018

110, E2865-E2874, 2013.

Sobek, S., DelSontro, T., Wongfun, N., and Wehrli, B.: Extreme organic carbon burial fuels intense methane bubbling in a temperate reservoir, Geophys Res Lett, 39, Artn L0140110.1029/2011gl050144, 2012.

Syvitski, J. P., Vörösmarty, C. J., Kettner, A. J., and Green, P.: Impact of humans on the flux of terrestrial sediment to the global coastal ocean, science, 308, 376-380, 2005.

Thornton, K. W., Kimmel, B. L., and Payne, F. E.: Reservoir limnology: ecological perspectives, John Wiley & Sons, 1990.

Toffolon, M., Siviglia, A., and Zolezzi, G.: Thermal wave dynamics in rivers affected by hydropeaking, Water Resources Research, 46, Artn W08536 10.1029/2009wr008234, 2010.

Tonina, D., and Buffington, J. M.: Effects of stream discharge, alluvial depth and bar amplitude on hyporheic flow in pool-riffle channels, Water resources research, 47, 2011.

Wang, C., Liu, S. L., Zhao, Q. H., Deng, L., and Dong, S. K.: Spatial variation and contamination assessment of heavy metals in sediments in the Manwan Reservoir, Lancang River, Ecotox Environ Safe, 82, 32-39, 10.1016/j.ecoenv.2012.05.006, 2012.

Wang, X. W., Li, X. Z., Hu, Y. M., Lv, J. J., Sun, J., Li, Z. M., and Wu, Z. F.: Effect of temperature and moisture on soil organic carbon mineralization of predominantly permafrost peatland in the Great Hing'an Mountains, Northeastern China, Journal of Environmental Sciences, 22, 1057-1066, 10.1016/S1001-0742(09)60217-5, 2010.

Watanabe, T., Kimura, M., and Asakawa, S.: Dynamics of methanogenic archaeal communities based on rRNA analysis and their relation to methanogenic activity in Japanese paddy field soils, Soil Biol Biochem, 39, 2877-2887, 10.1016/j.soilbio.2007.05.030, 2007.

Wilkinson, J., Maeck, A., Alshboul, Z., and Lorke, A.: Continuous seasonal river ebullition measurements linked to sediment methane formation, Environmental science & technology, 49, 13121-13129, 2015.

Wuebbles, D. J., and Hayhoe, K.: Atmospheric methane and global change, Earth-Sci Rev, 57, 177-210, 2002.

Yang, L., Lu, F., Wang, X., Duan, X., Song, W., Sun, B., Zhang, Q., and Zhou, Y.: Spatial and seasonal variability of diffusive methane emissions from the Three Gorges Reservoir, Journal of Geophysical Research: Biogeosciences, 118, 471-481, 2013.

Yang, Y. Y., Li, N. N., Wang, W., Li, B. X., Xie, S. G., and Liu, Y.: Vertical profiles of sediment methanogenic potential and communities in two plateau freshwater lakes, Biogeosciences, 14, 341-351, 10.5194/bg-14-341-2017, 2017.

Zarnetske, J. P., Haggerty, R., Wondzell, S. M., and Baker, M. A.: Labile dissolved organic carbon supply limits hyporheic denitrification, Journal of Geophysical Research: Biogeosciences, 116, 2011a.

Zarnetske, J. P., Haggerty, R., Wondzell, S. M., and Baker, M. A.: Labile dissolved organic carbon supply limits hyporheic denitrification, Journal of Geophysical Research, 116, 10.1029/2011jg001730, 2011b.

Biogeosciences Discuss., https://doi.org/10.5194/bg-2018-380
Manuscript under review for journal Biogeosciences
Discussion started: 13 September 2018

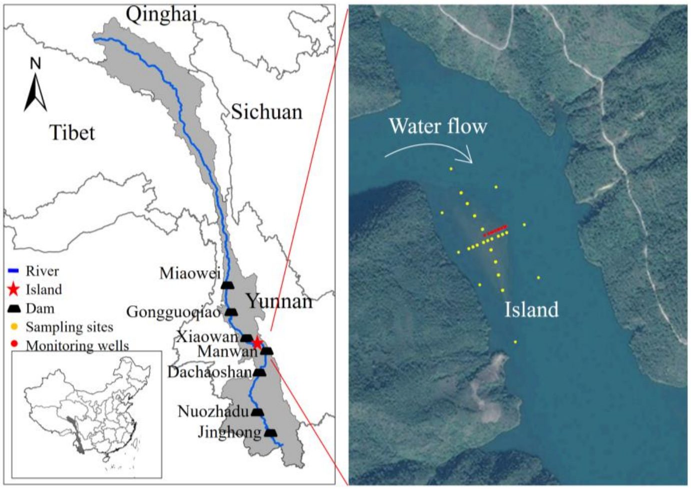

Fig. 1 Map of the studied island in Manwan reservoir, Lancang-Mekong River.

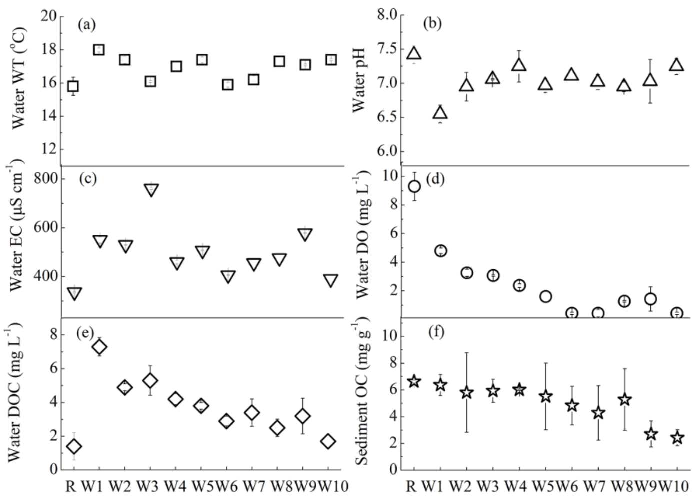

Fig. 2 Physicochemical properties of the island and reservoir, including water (a) WT, (b) pH, (c) EC, (d) DO, (e) DOC, and (f) sediment OC. Solid symbols represent the physicochemical properties of the reservoir. WT = water temperature, EC = electrical conductivity, DO = dissolved oxygen, DOC = dissolved oxygen carbon, OC = organic carbon, R = reservoir, W = monitoring wells. Error bars indicate standard deviations.

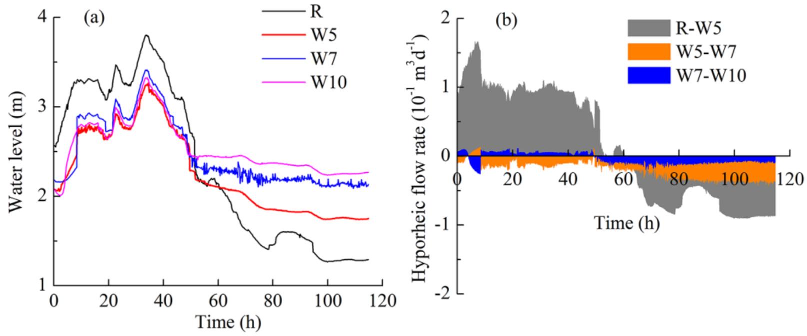

Fig. 3 Vertical water level fluctuation (a) and horizontal hyporheic flow rate (b). R = reservoir, W = monitoring wells. Positive fluxes indicate net flow from the reservoir to island, whereas negative values indicate net flow from the island to reservoir.

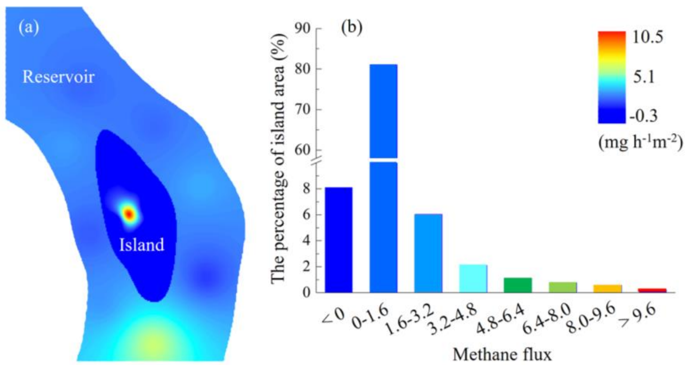

Fig. 4 Methane emissions from the island and reservoir. (a) Spatial pattern of methane emissions; (b) Percentage of the island area emitting methane at a certain flux. Methane fluxes were interpolated separately for the island and reservoir.

Biogeosciences Discuss., https://doi.org/10.5194/bg-2018-380
Manuscript under review for journal Biogeosciences
Discussion started: 13 September 2018

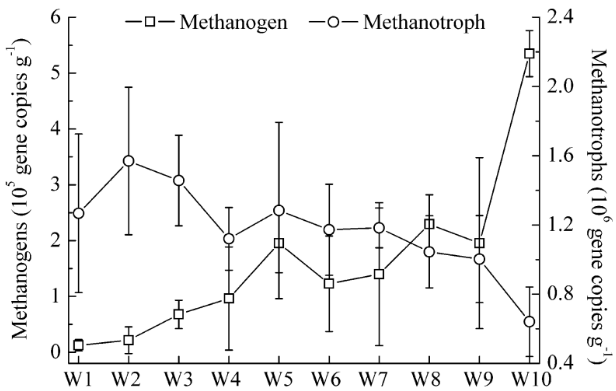

Fig. 5 Abundances of sediment methanogens and methanotrophs in the island. W= monitoring wells. Error bars indicate standard deviations.